Multiplet effects in the electronic structure of intermediate-valence compounds

P. Thunström,[1,*] I. Di Marco,[1,2] A. Grechnev,[3] S. Lebègue,[4] M. I. Katsnelson,[2] A. Svane,[5] and O. Eriksson[1]
[1]*Department of Physics and Materials Science, Uppsala University, Box 530, SE-75121, Uppsala, Sweden*
[2]*Institute for Molecules and Materials, Radboud University Nijmegen, NL-6525 ED Nijmegen, The Netherlands*
[3]*B. Verkin Institute for Low Temperature Physics and Engineering, 47 Lenin Avenue, Kharkov, Ukraine*
[4]*Laboratoire de Cristallographie, Résonance Magnétique et Modélisations (CRM2, UMR CNRS 7036) Institut Jean Barriol, Nancy Université, BP 239, Boulevard des Aiguillettes 54506 Vandoeuvre-lès-Nancy, France*
[5]*Department of Physics and Astronomy, University of Aarhus, DK-8000 Aarhus C, Denmark*
(Received 4 December 2008; revised manuscript received 23 February 2009; published 10 April 2009)

We present an implementation of the Hubbard-I approximation based on the exact solution of the atomic many-body problem incorporated in a full-potential linear muffin-tin orbital method of density-functional theory. Comparison between calculated and measured x-ray photoemission spectra reveal a good agreement for intermediate valence systems in open crystal structures such as $YbInCu_4$, SmB_6, and YbB_{12}. Spectral features of the unoccupied states of SmB_6 are predicted.

DOI: 10.1103/PhysRevB.79.165104 PACS number(s): 71.28.+d, 71.15.Qe

I. INTRODUCTION

The partially filled f-electron states in pure $4f$ and $5f$ metals usually form either localized atomiclike shells, e.g., in rare-earth elements,[1] or delocalized valence-band states, e.g., in light actinides.[2] However, the f electrons in their compounds often lie in between these two extremes. They can at the same time demonstrate bandlike behavior, by showing a small dispersion and contributing to the chemical binding and atomiclike behavior by giving rise to a rich multiplet structure in the excitation spectrum. Furthermore, a Kondo-like resonance often occurs in the meV energy scale around the Fermi level.[3] The complex competition between itinerant and localized electronic behavior leads to very interesting physical effects in many f-electron materials, such as intermediate valence (IV) systems[4–6] which have ground states where the f manifold rapidly fluctuates between the f^n and f^{n+1} configuration.

IV systems are sometimes metallic down to very low temperatures with ground states which can be described as paramagnetic Fermi liquids.[7,8] In this paper we consider three IV systems, $YbInCu_4$, YbB_{12}, and SmB_6, which all break this rule as the temperature is lowered. At ambient pressure, $YbInCu_4$ undergoes a first-order isostructural electronic phase transition at $T_c \approx 40$ K, which causes the electrical resistivity and the effective magnetic moment to drop by an order of magnitude.[9] YbB_{12} and SmB_6 on the other hand are classical examples of narrow-gap semiconductors which develop a band gap on the order of 10 meV as the temperature is lowered.[3] From theoretical point of view they are considered excitonic insulators[10–12] or Kondo insulators.[3]

$YbInCu_4$, YbB_{12}, and SmB_6 have been thoroughly studied by, for example, photoemission,[13–19] resonant inelastic x-ray scattering,[19–21] electrical transport,[22,23] neutron-scattering,[24–27] Mössbauer,[28–30] and optical[31–33] measurements.

Although the anomalous properties of these materials have been known for decades[9,34–37] the underlying mechanism and relation to the IV ground state is still under discussion.[11,12,20,24,38–42] Much of the effort has been centered around the description of the electronic structure in the meV energy scale close to the Fermi level. The electronic structure on the eV scale, describing the rich multiplet structures seen in photoemission experiments, has received substantially less attention although a full description of the problem requires both. This large scale electronic structure has so far only been addressed using the local density approximation[43–45] (LDA) and the LDA+U (Refs. 46 and 47) approach. It is worth noting that in Ref. 47 an atomic multiplet spectrum was positioned on top of the LDA+U density of states, in order to simulate the experimental multiplet structures. The poor agreement between the density of states from a regular LDA or LDA+U calculation and the observed photoemission spectrum of these materials highlights the need to include a more accurate description of the strong electron-electron correlations in the electronic structure calculations, especially if any post-processing procedure interprets the Kohn-Sham quasiparticles as real electronic excitation. The aim of this paper is to focus on the electronic structure on the eV scale and to find an accurate description of the multiplet structure.

The clear evidence of strong electron-electron correlations in $YbInCu_4$, YbB_{12}, and SmB_6 suggests that an accurate description of their electronic structure needs to go beyond the LDA. The LDA+Hubbard-I approximation[48,49] has been shown to give an adequate description of localized f-electron systems such as various Lanthanide and Actinide compounds.[50–53] The calculations of Refs. 50–53 were performed using a linear muffin-tin orbitals (LMTO) basis set in the atomic sphere approximation (ASA), which is unfortunately not reliable for materials with open crystal structures such as $YbInCu_4$, YbB_{12}, and SmB_6. In the present work we present a full-potential (FP) implementation of the Hubbard-I approximation. It is incorporated in the dynamical mean-field Theory[54–59] (DMFT) code described in Refs. 60 and 61 which is based on the FP-LMTO code RSPT.[62] We should mention that the Hubbard-I approximation (HIA) has previously been implemented in a FP-LMTO (Ref. 63) and a linear augmented plane waves[64] code.

The paper is organized as follows: in Sec. II we quickly review how the self-energy is obtained in the Hubbard-I approximation. The main results of our calculations of

$YbInCu_4$, YbB_{12}, and SmB_6 and the comparison with experimental data are found in Sec. III, followed by the conclusions in Sec. IV.

II. METHOD

The HIA combines the many-body effects necessary to describe localized atomiclike states, in our case the $4f$ states of Yb and Sm, with the one-electron picture needed to treat wide bands formed by delocalized valence electron states. It can be formulated as a reduced LDA+DMFT scheme where the local self-energy is obtained from an atomic calculation instead of a self-consistent DMFT cycle.[54,55]

The atomic model used in HIA is built around an Hamiltonian that describes only the correlated states of a single ion at a given site R,

$$H_R^{\mathrm{at}} = H_{0R}^{\mathrm{at}} + \frac{1}{2}\sum_{\lambda_j} U^R_{\lambda_1\lambda_2\lambda_3\lambda_4} c^\dagger_{R,\lambda_1} c^\dagger_{R,\lambda_2} c_{R,\lambda_3} c_{R,\lambda_4} - \mu_{\mathrm{at}} \sum_{\lambda} c^\dagger_{R,\lambda} c_{R,\lambda}. \tag{1}$$

Here the index λ_j labels the correlated orbitals [for f orbitals $\lambda=(m_l,\sigma)=1,\ldots,14$] and $c^\dagger_\lambda$ and c_λ are the corresponding creation and annihilation operators.

H_{0R}^{at} contains the single-particle LDA Hamiltonian, calculated without spin-orbit coupling, projected onto the correlated states. The spin-orbit coupling is instead added explicitly as a second term,

$$H_{0R}^{\mathrm{at}} = \sum_{\lambda_1\lambda_2} \langle R\lambda_1 | h_{\mathrm{LDA}} + \xi \mathbf{l}\cdot\mathbf{s} | R\lambda_2\rangle c^\dagger_{R,\lambda_1} c_{R,\lambda_2} \tag{2}$$

where h_{LDA} is the LDA Hamiltonian, ξ is the spin-orbit constant, $\mathbf{l}$ and $\mathbf{s}$ are the one-electron orbital moment and spin operators, and $\{|R,\lambda\rangle\}$ are correlated states at site R. The projection onto the correlated orbitals removes all off-diagonal "hopping" terms to states orthogonal to the correlated orbitals at site R but keeps the crystal-field effects. The site index R is from here on implicit.

The second term in Eq. (1) describes the electron-electron interaction, with the matrix element

$$U_{\lambda_1\lambda_2\lambda_3\lambda_4} = \int\int \frac{\phi^*_{\lambda_1}(\mathbf{r})\phi^*_{\lambda_2}(\mathbf{r}')\phi_{\lambda_3}(\mathbf{r}')\phi_{\lambda_4}(\mathbf{r})}{|\mathbf{r}-\mathbf{r}'|} d\mathbf{r}d\mathbf{r}' = \sum_\ell a_\ell(\lambda_1,\lambda_2,\lambda_3,\lambda_4) F^\ell, \tag{3}$$

where $\phi_m(\mathbf{r})$ are the correlated orbitals. In the second equality of Eq. (3) the Coulomb integrals are expressed in terms of Slater integrals F^ℓ and vector coupling coefficients a_ℓ.[65] The U matrix is determined completely by four parameters F^ℓ, $\ell=0,2,4,6$. The values of the parameters F^ℓ and ξ are determined in an *ab initio* way by radial integration of the f partial waves of a self-consistent LDA calculation.[66]

The last term in Eq. (1) contains the chemical potential μ_{at} which is used to embed the atom in the solid. The chemical potential is also used to cancel the energy contribution from the double counting of the one-body terms of the Coulomb interaction, as some of these terms are already included in H_0^{at}. How to obtain an accurate double-counting correction in an LDA+HIA scheme is still an open question, so in the present model we treat the chemical potential as an adjustable parameter.

The atomic Hamiltonian is diagonalized in the complete space spanned by all the Slater determinants of a given f^n configuration. In addition to the f^n configurations found in the mixed ground state, also the neighboring $f^{n\pm1}$ configurations must be included in the calculation to account for possible excitations. From the eigenvalues E_ν and eigenvectors $|\nu\rangle$ of the atomic Hamiltonian one can construct a local one-particle Green's function,

$$G^{\mathrm{at}}_{\lambda\lambda'}(\omega) = \frac{1}{Z}\sum_{\nu_1\nu_2} \frac{\langle\nu_1|c_\lambda|\nu_2\rangle\langle\nu_2|c^\dagger_{\lambda'}|\nu_1\rangle}{\omega + E_{\nu_1} - E_{\nu_2}} (e^{-\beta E_{\nu_1}} + e^{-\beta E_{\nu_2}}), \tag{4}$$

where ω belongs to the upper complex half-plane, $\beta = 1/k_BT$, and T is temperature. The atomic self-energy $\Sigma^{at}(\omega)$ is then obtained from

$$\Sigma^{\mathrm{at}}(\omega) = \omega - H_0^{\mathrm{at}} - (G^{\mathrm{at}})^{-1}(\omega). \tag{5}$$

The HIA can be incorporated into the DMFT scheme by replacing the local self-energy $\Sigma_R(\omega)$ of the corresponding single impurity problem with $\Sigma^{\mathrm{at}}(\omega)$, which effectively reduces the DMFT cycle to a "one shot" procedure.[67] The local self-energy obtained from the HIA solver can then be used as described in Ref. 60 to construct a partial density of the correlated states, which can be directly compared with spectra from high-energy photoemission and inverse photoemission spectroscopy.[68,69] At lower photon energies the importance of surface and scattering effects increases and the calculation of the theoretical spectrum should then take these effects into account explicitly.[69–71]

For this study HIA was implemented as an additional impurity solver in the LDA+DMFT code "BRIANNA" of Ref. 60. BRIANNA is built on top of the FP-LMTO code RSPT,[62,72] which allows us to calculate materials with any type of crystal structure (open or close packed). The correlated orbitals were set to be the (orthonormal) heads of the f-electron LMTO basis functions.[60,62]

III. RESULTS

As pointed out in Sec. II, the construction of the atomic Hamiltonian used in HIA requires a number of parameters such as the spin-orbit coupling parameter ξ, and the Slater integrals F^0, F^2, F^4, and F^6. The values of these parameters, except for F^0 (also known as the "Hubbard U" parameter), are obtained from *ab initio* calculations and can be found in Table I. The physically relevant value of the first Slater integral F^0 is reduced from the bare value given by Eq. (3) due to the screening from non-f-electrons,[73] and is set to be 8 eV for all compounds in the present study. The energy of an N-electron state depends on the value of F^0 as $F^0N(N-1)/2$. Since this contribution only depends on the number of electrons, a correction to the value of F^0 gives the same shift in energy for all the states within a f^n configuration. The

TABLE I. The values of the parameters in atomic Hamiltonian (1), obtained *ab initio* from radial integration of the f-partial waves of a self-consistent LDA calculation. F^0 is set to be 8 eV for all the compounds in the present study. The chemical potential is set to give the experimental occupation in the atomic problem.

	F^2 (eV)	F^4 (eV)	F^6 (eV)	ξ (eV)	μ_{at} (eV)
$YbInCu_4$	15.66	9.75	6.99	0.3888	96.8
YbB_{12}	15.83	9.86	7.08	0.3925	96.7
SmB_6	12.40	7.70	5.52	0.1635	36.1

form of the multiplets in the excitation spectra, corresponding to $f^n \rightarrow f^{n\pm1}$ transitions, remains therefore unchanged up to a rigid shift in energy. The chemical potential was set to give the experimental[13,14,19] intermediate valence occupation in the atomic problem. The values of the chemical potential used in the calculations are listed in Table I. The calculations were performed for $T=630$ K. The experimental photoemission spectra which are shown in Figs. 1 and 3 have been corrected to show only the contribution from the f-electron states. For details about these corrections see Refs. 19 and 13. The spectrum of YbB_{12} in Fig. 2 was taken at 700 eV, which makes the photoionization cross sections of B $2p$ negligible in comparison to Yb $4f$.

A. $YbInCu_4$

To begin our study of the intermediate valence compounds, we consider $YbInCu_4$. It has the $MnSnCu_4$-type crystal structure derived from space group 216 ($F\bar{4}3m$) with lattice parameter $a=7.15$ Å, and In in Wyckoff position $4a$, Yb in $4c$, and Cu in $16e$, with parameter $x=0.625$. The ground-state configuration of Yb in $YbInCu_4$ is a mixture of f^{13} and f^{14}, which gives rise to an x-ray photoemission spectroscopy (XPS) spectrum that contains both f^{14} to f^{13} and f^{13} to f^{12} transitions.

The partial density of states from the LDA+HIA calculation is shown in the upper panel of Fig. 1, together with an experimental photoemission spectrum from Ref. 19. The agreement is excellent, and all the major peaks observed in the experiment are reproduced by our calculations. The double peak structure between −2 eV and 0 eV corresponds to f^{14} to f^{13} transitions where the final states $^2F_{5/2}$ and $^2F_{7/2}$ are separated in energy by 1.3 eV due to the spin-orbit interaction. Hybridization effects cause the latter peak to broaden and shift by +0.2 eV compared to the bare atomic level. At higher binding energies, between −12 eV to −5 eV, the structures are caused by f^{13} to f^{12} transitions.

Three distinct peaks are observed in the experimental spectrum between −6 eV and −9 eV, which are related to final states of ^3H, ^3F, and ^1G characters. However, due to the large spin-orbit coupling, these peaks are shifted by up to 2 eV and split into the complex six-peak structure clearly seen in both the experimental and theoretical spectrum. Since the spin-orbit coupling does not conserve the L and S quantum numbers, the spectroscopic notation in Fig. 1 becomes only approximate except for the J quantum number. Between

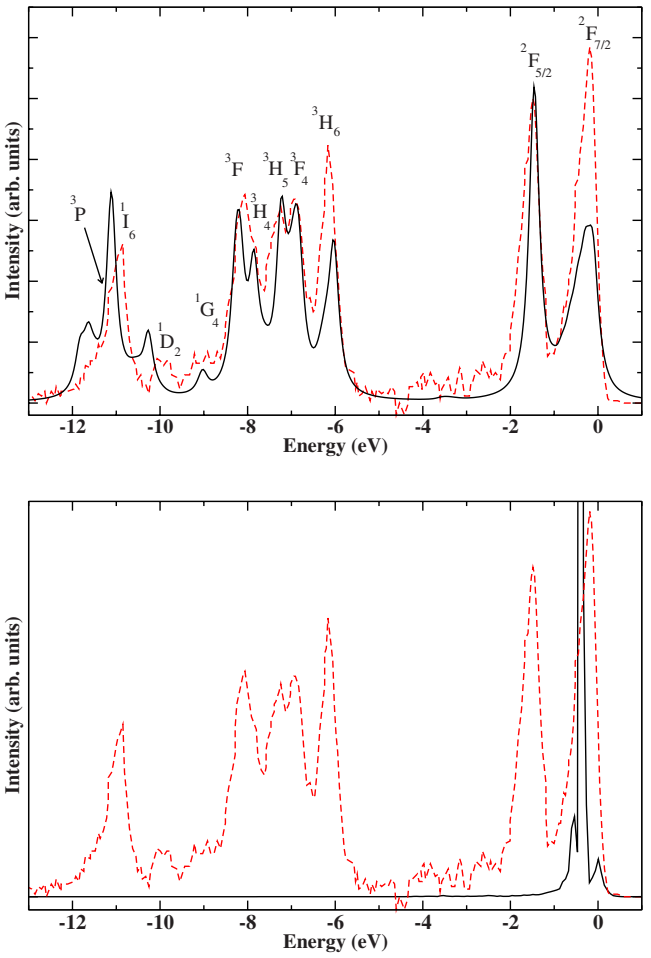

FIG. 1. (Color online) Partial density of states from LDA+HIA (full black line) and experimental photoemission spectrum from Ref. 19 (dashed red line) of the Yb f electron states in $YbInCu_4$ (upper panel). The f-projected density of states from the LDA calculation (full black line) with the measured photoemission spectrum (lower panel).

−12 eV and −10 eV three peaks are seen in the calculated spectrum, which can be associated with the ^1D, ^1I, and ^3P final states. These peaks are shifted and in the latter case also split by the spin-orbit coupling. Only the first two peaks are clearly visible in the experiment, while the ^3P appears as the shoulder around −11.5 eV. The experimental peak positions occur at slightly lower (~0.3 eV) binding energies compared to our calculation.

The lower panel of Fig. 1 shows the f-projected density of states for $YbInCu_4$ as calculated in the LDA, where the f manifold is treated as one-electron band states. This leads to a concentration of all the f-electron spectral weight in a narrow peak at the Fermi level, which is in sharp contrast to the experimental spectrum that shows the f-spectral weight distributed over a 12 eV range.

B. YbB_{12}

The next intermediate valence compound in our study is YbB_{12}. It has the UB_{12}-type crystal structure given by space

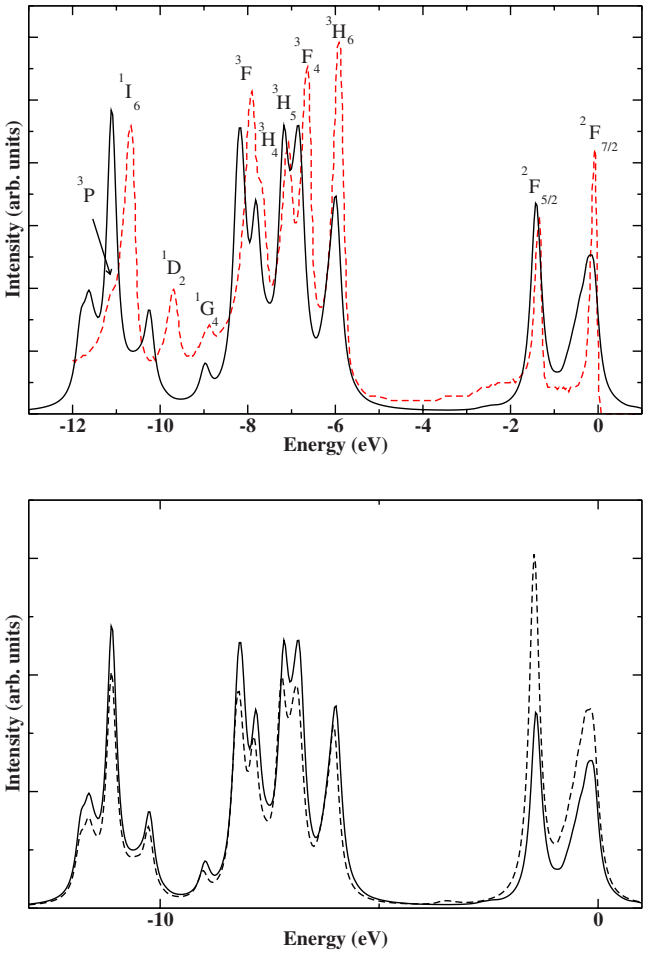

FIG. 2. (Color online) Partial density of states from LDA +HIA (full black line) and experimental photoemission spectrum from Ref. 14 (dashed red line) of the Yb f electron states in YbB_{12} (upper panel). The lower panel shows a comparison of the partial density of states from LDA+HIA of YbB_{12} (full black line) and $YbInCu_4$ (dashed black line).

group 225 ($Fm\bar{3}m$) with Yb in Wyckoff position 4a and B in 48i with parameter $y=0.166$ and lattice constant $a=7.464$ Å. The ground-state configuration of Yb is a mixture of f^{13} and f^{14}, similar to that found in $YbInCu_4$, which gives rise to striking similarities in their spectra, as seen in lower panel of Fig. 2. Our calculation reproduces all the main features in the XPS spectrum, as shown in the upper panel of Fig. 2. Like in $YbInCu_4$ the peaks between −13 eV and −9.5 eV are found to be shifted by approximately +0.4 eV. Compared to the case of $YbInCu_4$, the experiment clearly resolves all the spin-orbit induced splittings including the split-off peak at −9 eV.

C. SmB_6

SmB_6 has the CaB_6-type crystal structure given by space group 211 ($Pn\bar{3}m$) and lattice parameter $a=4.1333$ Å. Sm occupies Wyckoff position 1a, and B occupies position 6f with parameter $x=0.2$. The ground-state configuration of Sm in SmB_6 is a mixture of f^5 and f^6; therefore the observed

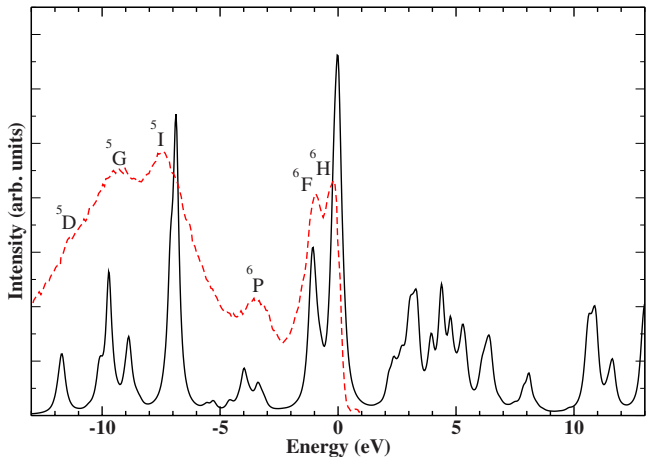

FIG. 3. (Color online) Partial density of states from LDA +HIA (full black line) and experimental photoemission spectrum from Ref. 13 (dashed red line) of the Sm f electron states in SmB_6.

XPS spectrum corresponds to excitations from f^6 to f^5 and f^5 to f^4.

Figure 3 shows the partial density of states for the Sm 4f orbitals in SmB_6 obtained from LDA+HIA. A photoemission spectrum from Ref. 13 is included for comparison. The overall agreement is quite good. The peaks between −5 eV and 0 eV corresponds to excitations from f^6 to f^5 with final states ^6P, ^6F, and ^6H. The ^6F and ^6H peaks at 0 eV and −1.1 eV compare fairly well with the features in the experimental XPS spectrum, considering that the photoemission spectroscopy only shows the occupied part of the spectrum. The structure around −4 eV may be identified with the ^6P final state. Its binding energy in the calculation is approximately 0.4 eV larger than the binding energy of the corresponding experimental shoulder. The structures between −12 eV and −5 eV are associated with the excitations from f^5 to f^4 with final states ^5D, ^5G, ^5F, and ^5I. The central ^5G and ^5F peaks are positioned at 9.7 and 8.9 eV which agrees fairly well with the position of the lower of the two peaks observed in experiment. The ^5D is hardly visible in the experiment, while the ^5I peak may be identified with the experimental peak at −7.5 eV (shifted by +0.7 eV). The theoretical curve shows a number of multipletlike features in the unoccupied states, which in the lack of experimental observations, must be viewed as a prediction.

IV. CONCLUSIONS

We have calculated the electronic structure of $YbInCu_4$, YbB_{12}, and SmB_6 using a new FP-LMTO LDA+HIA implementation. The theoretical partial densities of the correlated states and the measured photoemission spectra presented in Sec. III show an overall excellent agreement. All major peaks are reproduced and their positions lie within a few tenths of an electron volt of the experimental positions. These results confirm that the atomic picture of isolated rare-earth ions as implemented in the FP-LMTO LDA+HIA approach accurately describes the 4f manifold in Yb and Sm systems for which the 4f states exhibit strong correlations

but very weak hybridization, as is the case in the presently studied open crystal structures. It should be noted that the main advantage with implementing the Hubbard-I approximation in a full-potential electronic structure code is that open crystal structures can be considered.

The small discrepancy between observations and theory in peak positions is likely caused by an overestimation of the Slater integrals since the current *ab initio* calculation does not include an explicit screening in the evaluation of the Slater integrals. Replacing this *ab initio* calculation with some fitting procedure would, naturally, produce a closer agreement with the fitted spectrum, but severely restrict the predictability power of the method.

The experimental photoemission spectra as well as the theoretical partial density of states for $YbInCu_4$ and YbB_{12} show striking similarities. The theoretical partial density of states for SmB_6 shows similar features to the spectral f density for the intermediate valence compound SmS, obtained through a model Hamiltonian approach in Ref. 74. These similarities indicate that, for the compounds studied in the present paper, the chemical environment of the f manifold mainly affects its occupancy, and not so much the relative energies of the many-body states within a given f^n configuration.

To settle the debate concerning the origin of the ground state in IV systems and whether or not coherent states which have heavy-fermion characters are formed, one would need to accurately describe the electronic structure on a large energy scale, with all the atomiclike multiplets in the density of states, as well as on a minute scale, implying getting all small details of the order of meV close to the Fermi level correctly, all within a single model. Since LDA+HIA can describe the larger energy scale very well it could hopefully serve as a starting point in some refined scheme where the smaller energy scales are probed by a Quantum Monte Carlo DMFT solver or perhaps by including ligand orbitals in a cluster HIA calculation.

ACKNOWLEDGMENTS

Two of the authors (P.T. and O.E.) would like to acknowledge support from the Swedish Research Council (VR), Energimyndigheten, and the Swedish National Infrastructure for Computing (SNIC). I.D.M. would like to acknowledge support from Stichting Nationale Computerfaciliteiten (National Computing Facilities Foundation, NCF) and the Nederlandse Organisatie voor Wetenschappelijk Onderzoek (Netherlands Organization for Scientific Research, NWO). S.L. acknowledges the financial support from ANR PNANO through Grants No. ANR-06-NANO-053-02 and ANR-BLAN07-1-186138.

*patrik.thunstrom@fysik.uu.se

[1] S. Vonsovsky, *Magnetism* (Wiley, New York, 1974), Vol. 2.
[2] A. Freeman and D. Koelling, in *The Actinides: Electronic Structure and Related Properties*, edited by A. Freeman and J. Darby (Academic, New York, 1974), Vol. 1, p. 51.
[3] P. S. Riseborough, Adv. Phys. **49**, 257 (2000).
[4] R. Parks, *Valence Instabilities and Related Narrow-Band Phenomena* (Plenum Press, New York, 1977).
[5] J. Lawrence, P. Riseborough, and R. Parks, Rep. Prog. Phys. **44**, 1 (1981).
[6] *Proceedings of the International Conference on Valence Fluctuations*, edited by E. Müller-Hartmann, B. Roden, and D. Wohlleben (Elsevier, New York, 1985), Vols. 47-48.
[7] C. M. Varma, Rev. Mod. Phys. **48**, 219 (1976).
[8] P. Wachter, *Handbook on the Physics and Chemistry of Rare Earth* (Elsevier, New York, 1994), Vol. 19, pp. 177–382.
[9] I. Felner and I. Nowik, Phys. Rev. B **33**, 617 (1986).
[10] K. W. H. Stevens, J. Phys. C **9**, 1417 (1976).
[11] V. Y. Irkhin and M. I. Katsnelson, Solid State Commun. **58**, 881 (1986).
[12] V. Y. Irkhin and M. I. Katsnelson, J. Phys. C **17**, L699 (1984).
[13] J. N. Chazalviel, M. Campagna, G. K. Wertheim, and P. H. Schmidt, Phys. Rev. B **14**, 4586 (1976).
[14] A. Shigemoto, S. Imada, A. Sekiyama, A. Yamasaki, A. Irizawa, T. Muro, Y. Saitoh, F. Iga, T. Takabatake, and S. Suga, J. Electron Spectrosc. Relat. Phenom. **144-147**, 671 (2005).
[15] T. Susaki *et al.*, Phys. Rev. Lett. **82**, 992 (1999).
[16] F. Reinert, R. Claessen, G. Nicolay, D. Ehm, S. Hüfner, W. P. Ellis, G.-H. Gweon, J. W. Allen, B. Kindler, and W. Assmus, Phys. Rev. B **58**, 12808 (1998).
[17] D. P. Moore, J. J. Joyce, A. J. Arko, J. L. Sarrao, L. Morales, H. Hochst, and Y. D. Chuang, Phys. Rev. B **62**, 16492 (2000).
[18] H. Sato *et al.*, Phys. Rev. Lett. **93**, 246404 (2004).
[19] L. Moreschini *et al.*, Phys. Rev. B **75**, 035113 (2007).
[20] H. Yamaoka, N. Tsujii, K. Yamamoto, A. M. Vlaicu, H. Oohashi, H. Yoshikawa, T. Tochio, Y. Ito, A. Chainani, and S. Shin, Phys. Rev. B **78**, 045127 (2008).
[21] C. Dallera, M. Grioni, A. Shukla, G. Vankó, J. L. Sarrao, J. P. Rueff, and D. L. Cox, Phys. Rev. Lett. **88**, 196403 (2002).
[22] A. Menth, E. Buehler, and T. H. Geballe, Phys. Rev. Lett. **22**, 295 (1969).
[23] F. Iga, N. Shimizu, and T. Takabatake, J. Magn. Magn. Mater. **177-181**, 337 (1998).
[24] K. S. Nemkovski, J.-M. Mignot, P. A. Alekseev, A. S. Ivanov, E. V. Nefeodova, A. V. Rybina, L.-P. Regnault, F. Iga, and T. Takabatake, Phys. Rev. Lett. **99**, 137204 (2007).
[25] P. A. Alekseev, V. N. Lazukov, J. M. Mignot, and I. P. Sadikov, Physica B **281-282**, 34 (2000).
[26] A. Severing, E. Gratz, B. Rainford, and K. Yoshimura, Physica B **163**, 409 (1990).
[27] J. M. Lawrence, S. M. Shapiro, J. L. Sarrao, and Z. Fisk, Phys. Rev. B **55**, 14467 (1997).
[28] R. L. Cohen, M. Eibschütz, and K. W. West, Phys. Rev. Lett. **24**, 383 (1970).
[29] A. Yaouanc, P. D. de Réotier, P. Bonville, G. Lebras, P. C. M. Gubbens, A. M. Mulders, and S. Kunii, Europhys. Lett. **47**, 247 (1999).
[30] I. Felner *et al.*, Phys. Rev. B **35**, 6956 (1987).

[31] G. Travaglini and P. Wachter, Phys. Rev. B **29**, 893 (1984).
[32] H. Okamura, S. Kimura, H. Shinozaki, T. Nanba, F. Iga, N. Shimizu, and T. Takabatake, Phys. Rev. B **58**, R7496 (1998).
[33] H. Okamura, T. Michizawa, T. Nanba, and T. Ebihara, Phys. Rev. B **75**, 041101(R) (2007).
[34] G. C. Allen and N. S. Hush, Prog. Inorg. Chem. **8**, 357 (1967).
[35] A. Jayaraman, V. Narayanamurti, E. Bucher, and R. G. Maines, Phys. Rev. Lett. **25**, 368 (1970).
[36] M. B. Maple and D. Wohlleben, Phys. Rev. Lett. **27**, 511 (1971).
[37] M. B. Robin and P. Day, Adv. Inorg. Chem. Radiochem. **10**, 247 (1968).
[38] L. M. Falicov and J. C. Kimball, Phys. Rev. Lett. **22**, 997 (1969).
[39] R. M. Martin and J. W. Allen, J. Appl. Phys. **50**, 7561 (1979).
[40] B. Bucher, Z. Schlesinger, P. C. Canfield, and Z. Fisk, Phys. Rev. Lett. **72**, 522 (1994).
[41] T. Kasuya, Physica B **223-224**, 402 (1996).
[42] J. C. Cooley, M. C. Aronson, Z. Fisk, and P. C. Canfield, Phys. Rev. Lett. **74**, 1629 (1995).
[43] H. Harima, S. Miyahara, and A. Yanase, Physica B **163**, 205 (1990).
[44] A. Yanase and H. Harima, Prog. Theor. Phys. **108**, 19 (1992).
[45] K. Takegahara and T. Kasuya, J. Phys. Soc. Jpn. **59**, 3299 (1990).
[46] T. Saso and H. Harima, J. Phys. Soc. Jpn. **72**, 1131 (2003).
[47] V. N. Antonov, B. N. Harmon, and A. N. Yaresko, Phys. Rev. B **66**, 165209 (2002).
[48] A. I. Lichtenstein and M. I. Katsnelson, Phys. Rev. B **57**, 6884 (1998).
[49] J. Hubbard, Proc. R. Soc. London, Ser. A. **276**, 238 (1963).
[50] A. Svane, Solid State Commun. **140**, 364 (2006).
[51] S. Lebègue, G. Santi, A. Svane, O. Bengone, M. I. Katsnelson, A. I. Lichtenstein, and O. Eriksson, Phys. Rev. B **72**, 245102 (2005).
[52] S. Lebègue, A. Svane, M. I. Katsnelson, A. I. Lichtenstein, and O. Eriksson, J. Phys.: Condens. Matter **18**, 6329 (2006).
[53] S. Lebègue, A. Svane, M. I. Katsnelson, A. I. Lichtenstein, and O. Eriksson, Phys. Rev. B **74**, 045114 (2006).
[54] K. Held, Adv. Phys. **56**, 829 (2007), 10.1080/00018730701619647.
[55] G. Kotliar, S. Y. Savrasov, K. Haule, V. S. Oudovenko, O. Parcollet, and C. A. Marianetti, Rev. Mod. Phys. **78**, 865 (2006).
[56] A. Georges, G. Kotliar, W. Krauth, and M. J. Rozenberg, Rev. Mod. Phys. **68**, 13 (1996).
[57] M. Katsnelson, V. Irkhin, L. Chioncel, A. Lichtenstein, and R. de Groot, Rev. Mod. Phys. **80**, 315 (2008).
[58] K. Held, V. Anisimov, V. Eyert, G. Keller, A. McMahan, I. Nekrasov, and D. Vollhardt, Adv. Solid State Phys. **43**, 267 (2003), 10.1007/b12017.
[59] G. Kotliar and D. Vollhardt, Phys. Today **57**, 53 (2004).
[60] A. Grechnev, I. Di Marco, M. I. Katsnelson, A. I. Lichtenstein, J. Wills, and O. Eriksson, Phys. Rev. B **76**, 035107 (2007).
[61] I. Di Marco, J. Minár, S. Chadov, M. Katsnelson, H. Ebert, and A. Lichtenstein, Phys. Rev. B **79**, 115111 (2009).
[62] J. Wills, O. Eriksson, M. Alouani, and D. Price, in *Electronic Structure and Physical Properies of Solids*, edited by H. Dreysse (Springer, New York, 2000), pp. 148–167.
[63] S. Y. Savrasov, V. Oudovenko, K. Haule, D. Villani, and G. Kotliar, Phys. Rev. B **71**, 115117 (2005).
[64] A. Shick, J. Kolorenc, L. Havela, V. Drchal, and T. Gouder, EPL **77**, 17003 (2007).
[65] B. Judd, *Operator Techniques in Atomic Spectroscopy* (Princeton University Press, Prinston, New Jersey, 1998).
[66] O. Eriksson, M. S. S. Brooks, and B. Johansson, Phys. Rev. B **41**, 7311 (1990).
[67] The authors humbly leave it to the reader to decide whether or not to refer to the Hubbard-I approximation as a DMFT scheme.
[68] C. N. Berglund and W. E. Spicer, Phys. Rev. **136**, A1030 (1964).
[69] C. Caroli, D. Lederer-Rozenblatt, B. Roulet, and D. Saint-James, Phys. Rev. B **8**, 4552 (1973).
[70] J. B. Pendry, Surf. Sci. **57**, 679 (1976).
[71] G. Borstel, Appl. Phys. A: Solid Surf. **38**, 193 (1985).
[72] URL: http://www.rspt.net/.
[73] V. I. Anisimov and O. Gunnarsson, Phys. Rev. B **43**, 7570 (1991).
[74] C. Lehner, M. Richter, and H. Eschrig, Phys. Rev. B **58**, 6807 (1998).